Journal of ELECTRONIC MATERIALS, Vol. 40, No. 5, 2011
DOI: 10.1007/s11664-010-1481-0

Thin-Film Thermoelectric Module for Power Generator Applications Using a Screen-Printing Method

HEON-BOK LEE,[1] HYUN JEONG YANG,[1] JU HYUNG WE,[1] KUKJOO KIM,[1] KYUNG CHEOL CHOI,[1] and BYUNG JIN CHO[1,2]

1.—Department of Electrical Engineering, KAIST, 335 Gwahak-Ro, Daejeon, Korea. 2.—e-mail: bjcho@ee.kaist.ac.kr

A new process for fabricating a low-cost thermoelectric module using a screen-printing method has been developed. Thermoelectric properties of screen-printed ZnSb films were investigated in an effort to develop a thermoelectric module with low cost per watt. The screen-printed Zn_xSb_{1-x} films showed a low carrier concentration and high Seebeck coefficient when x was in the range of 0.5 to 0.57 and the annealing temperature was kept below 550°C. When the annealing temperature was higher than 550°C, the carrier concentration of the Zn_xSb_{1-x} films reached that of a metal, leading to a decrease of the Seebeck coefficient. In the present experiment, the optimized carrier concentration of screen-printed ZnSb was $7 \times 10^{18}/cm^3$. The output voltage and power density of the ZnSb film were 10 mV and 0.17 mW/cm^2, respectively, at ΔT = 50 K. A thermoelectric module was produced using the proposed screen-printing approach with ZnSb and $CoSb_3$ as p-type and n-type thermoelectric materials, respectively, and copper as the pad metal.

Key words: Thermoelectronics, TE module, power generator, green technology, screen-printing

INTRODUCTION

Thermoelectric modules have been used in cooler applications and power generators on the basis of their capacity to accomplish direct conversion between thermal and electrical energy.[1] In the case of cooler applications, an electrical power source should be supplied to operate the thermoelectric module. Therefore, the coefficient of performance (COP), which is defined as the cooling capacity Q divided by the consumed electric power, is an important factor. If the COP is low, the thermoelectric module consumes excessive electric power. To reduce the operating cost, the thermoelectric module must accordingly have a high COP value.[2–6] The COP also has a direct relation with the thermoelectric figure of merit (ZT).[7] Therefore, recent research on thermoelectric modules has mainly focused on improving the ZT of materials.

On the other hand, in the case of generator applications, the cost per watt of the thermoelectric module is a more critical factor than the conversion efficiency if the thermal energy source is sufficient.[8–11] In this work, we focus on the development of a low-cost thermoelectric module for power generator applications. To this end, screen-printing technology, a simple and low-cost process that is suitable for mass production, has been adopted to deposit thermoelectric materials and metal pads. We investigated the screen-printing process and the thermoelectric properties of a screen-printed ZnSb film. As the base materials (Zn and Sb) are abundant, it is anticipated that this route can provide a nontoxic means of realizing a thermoelectric module with low cost per watt. We demonstrate a thermoelectric module using this screen-printing approach with ZnSb and $CoSb_3$ as p-type and n-type thermoelectric materials, respectively, and copper as the pad metal.

(Received May 30, 2010; accepted December 2, 2010; published online January 4, 2011)

THERMOELECTRIC PROPERTIES OF SCREEN-PRINTED ZN_XSB_{1-X} FILMS

ZnSb paste was made by mixing Zn and Sb powders, an organic vehicle, and a dispersant. The Zn and Sb powders were of 99.0% purity, and the size of the powder particles was 44 μm or below. α-Terpineol was used as a vehicle, and DisperBYK-110 was employed as a dispersant. Mixed Zn_xSb_{1-x} powder (10 g), 10 mL α-terpineol, and 1 mL DisperBYK-110 were mixed thoroughly using a ball-milling device for 1 day. The viscosity of the synthesized ZnSb paste was 0.2 Pa s. The Zn_xSb_{1-x} paste was then printed onto a SiO_2/silicon substrate by using a 325 mesh screen. The printed film was leveled for more than 10 min and dried at 100°C in air for 10 min. Finally, the film was annealed in a furnace tube in air ambient at various temperatures. The furnace annealing was a two-step annealing process: in the first step, solvent was removed at 300°C for 20 min, and the second step entailed the application of higher temperature for 10 min. Electrical and thermoelectric properties of the printed Zn_xSb_{1-x} film were measured using a Keithley 2700 data acquisition system.

Figure 1 shows a scanning electron microscopy (SEM) image of the cross-section of the annealed ZnSb film and its thermoelectric properties. The thickness of the printed ZnSb thermoelectric film was about 30 μm. Although the screen-printed ZnSb film was porous due to evaporation of the solvent during the annealing process, the film showed reasonable thermoelectric properties, as presented in Fig. 1. The screen-printed ZnSb film had a power factor ($S^2\sigma$) in the range from 10^{-3} W/mK^2 to 10^{-4} W/mK^2, which is similar to that of bulk ZnSb material. The composition ratio dependence of the thermoelectric properties of Zn_xSb_{1-x} films was investigated, and the results are shown in Fig. 2. In this case, Zn_xSb_{1-x} films were annealed at 480°C in air ambient. The highest power factor was found at a Zn content range of 50% (ZnSb phase) to 57% (Zn_4Sb_3 phase). Figure 3a, b shows the impact of annealing on the thermoelectric properties of Zn_xSb_{1-x} films at various temperatures. A relatively low carrier concentration and a high Seebeck coefficient were found when the Zn content was 50% to 57%. When the annealing temperature was higher than 550°C, the carrier concentration of the Zn_xSb_{1-x} films reached that of a metal, leading to a decrease of the Seebeck coefficient. Another point to be noted is that the ZnSb film annealed in a furnace tube was oxidized, because the annealing was carried out in an air ambient. Our Auger electron spectroscopy (AES) analysis showed that the oxygen percentage in the film was around 35% and 25% at the surface and middle of the ZnSb film, respectively, after furnace annealing. Therefore, the present ZnSb film is not pure ZnSb, but rather $Zn_xSb_yO_{1-x-y}$. In our experiments, the film annealed in an ambient with oxygen always provided better performance. The detailed mechanism and role of oxygen in screen-printed ZnSb are not fully understood at the moment and will be studied in future research. Although the correct expression of the film is $Zn_xSb_yO_{1-x-y}$, we use the notation Zn_xSb_{1-x} in this paper for simplicity and to avoid possible confusion.

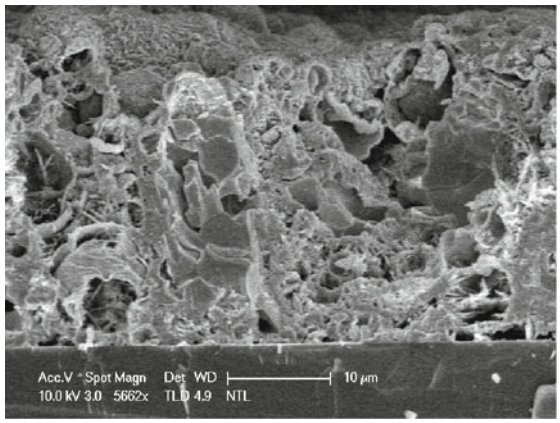

(a)

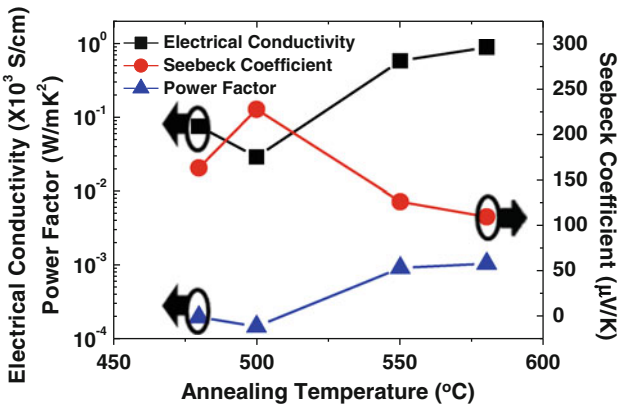

(b)

Fig. 1. (a) SEM image of the cross-section of an annealed ZnSb film, and (b) its thermoelectric properties.

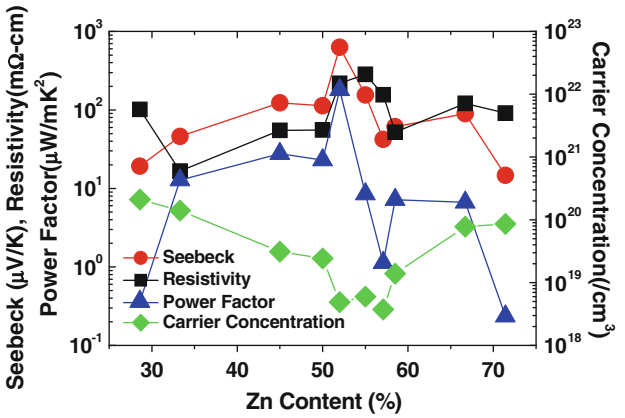

Fig. 2. The composition ratio dependence of thermoelectric properties of Zn_xSb_{1-x} films annealed at 480°C in air ambient.

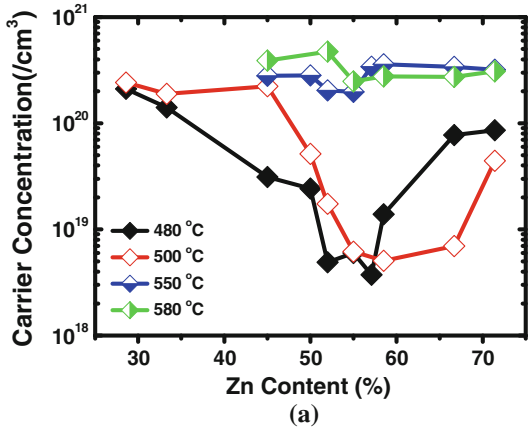

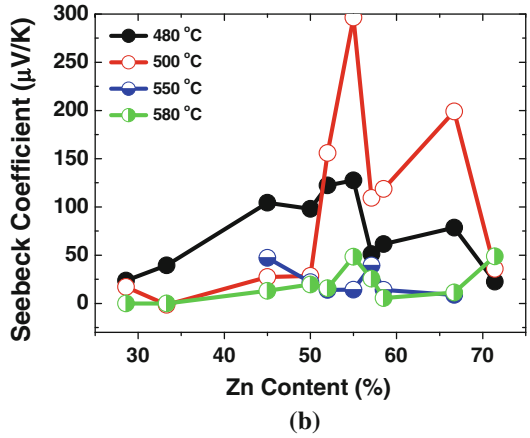

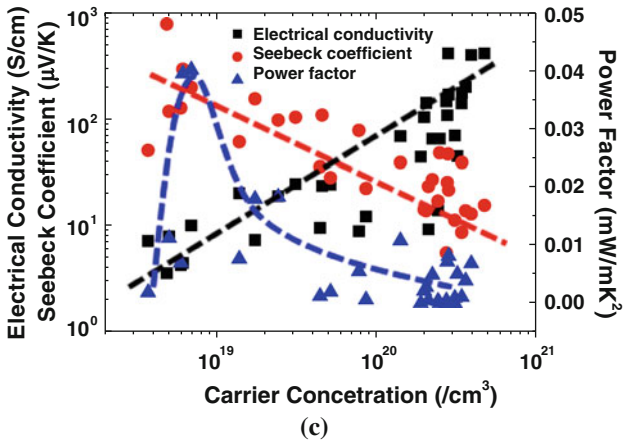

Fig. 3. (a) Carrier concentration and (b) Seebeck coefficient of Zn_xSb_{1-x} films annealed at different temperatures. (c) Thermoelectric properties of the screen-printed Zn_xSb_{1-x} film as a function of carrier concentration.

Figure 3c shows the thermoelectric properties of the Zn_xSb_{1-x} film as a function of carrier concentration. The ZnSb films showed a high electrical conductivity at high carrier concentrations and a high Seebeck coefficient at low carrier concentrations, consistent with previous reports on bulk ZnSb. In our experiment, the optimized carrier concentration of the screen-printed ZnSb was $7 \times 10^{18}/cm^3$.

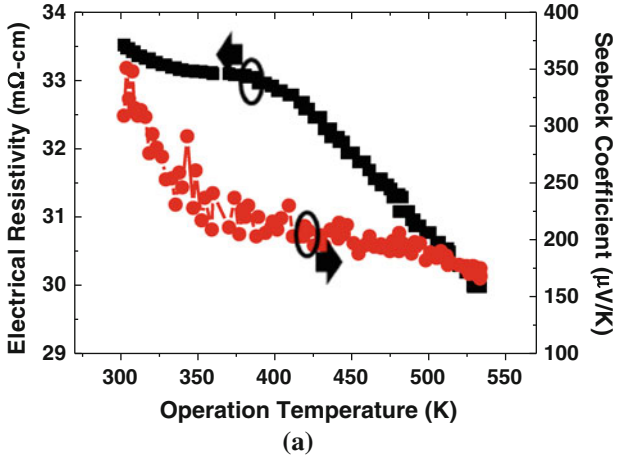

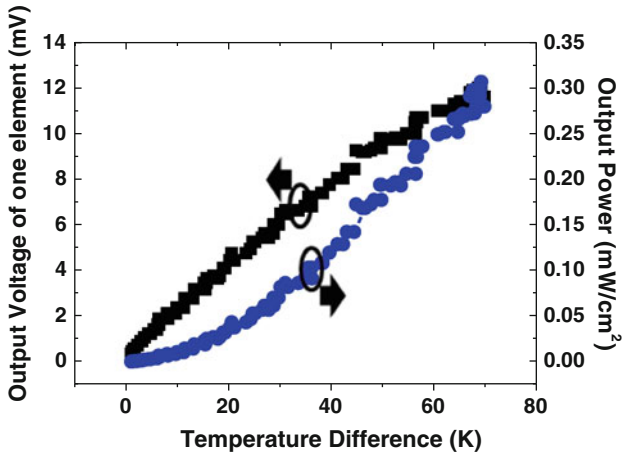

Fig. 4. (a) Electrical resistivity and Seebeck coefficient as a function of operation temperature. (b) Output voltage of one element and output power per unit area as a function of temperature difference. The ZnSb film was annealed at 500°C in air ambient in a furnace tube.

The power generation characteristics of the ZnSb film annealed at 500°C in air ambient in a furnace tube were investigated. Figure 4a shows the electrical resistivity and Seebeck coefficient as a function of the operation temperature, and Fig. 4b shows the output voltage of one element and output power per unit area as a function of the temperature difference. The electrical resistivity and Seebeck coefficient decrease as the operation temperature increases in a temperature range of 300 K to 550 K. The output power per unit area at a temperature difference of 50 K was 0.17 mW/cm^2. Although the output power was lower than that of a commercial thermoelectric module using Bi-Te materials, the cost per watt of the screen-printed ZnSb film will be lower, considering the raw material and fabrication process costs.

FABRICATION OF A THERMOELECTRIC MODULE USING SCREEN-PRINTING TECHNOLOGY

The suggested screen-printing technique is suitable for mass production as it is simple and

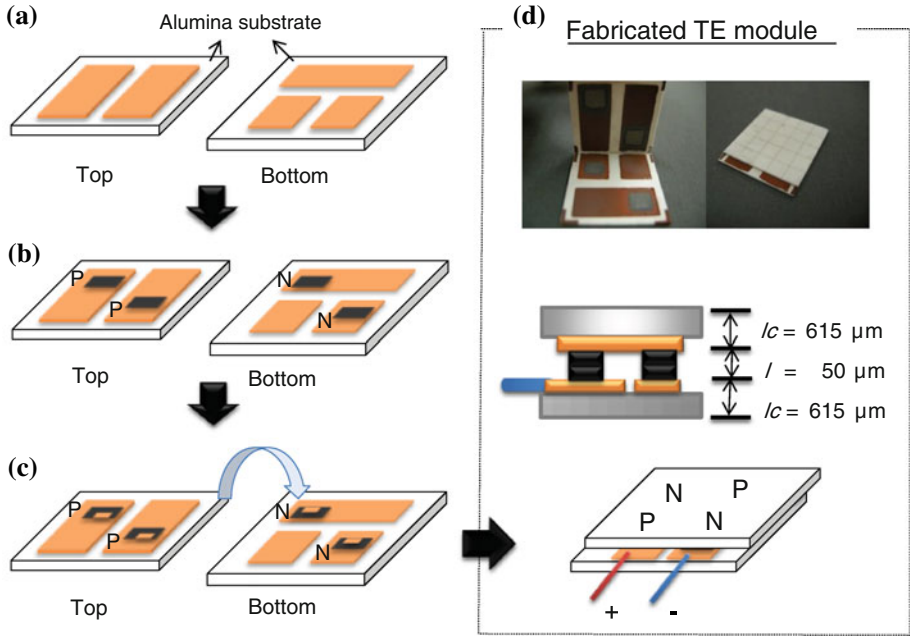

Fig. 5. Process flow of a thermoelectric module fabricated using screen-printing. (a) First step: Cu paste is deposited via screen-printing on an alumina substrate and annealed at 500°C for 10 min. (b) Second step: ZnSb is deposited on the top substrate as a *p*-type material, and $CoSb_3$ is deposited on the bottom substrate as an *n*-type material. The sample is then annealed at 500°C for 10 min. (c) Third step: the top and bottom substrate are bonded using Cu paste. (d) Photographs of fabricated thermoelectric module.

economical with capability for high throughput and large-area processing. Furthermore, this process is advantageous in terms of integration of layers, including other thermoelectric materials and pad metal, without requiring a lithography process. In this work, a thermoelectric module fabricated by screen-printing in conjunction with both *n*- and *p*-type thermoelectric materials and a pad metal was demonstrated. ZnSb and $CoSb_3$ were employed as *p*-type thermoelectric and *n*-type thermoelectric materials, and Cu was used as the pad metal. ZnSb and $CoSb_3$ pastes were composed of Zn, Sb, and Co powder, solvent, organic binder, and glass frit. All powders had 99.0% purity, and the size of the powder particle was 44 μm or below. Organic binder and glass frit were used to improve adhesion and viscosity. The viscosity of the ZnSb and $CoSb_3$ pastes were 7.2 Pa s and 8.1 Pa s, respectively. Cu paste was also composed of Cu powder, solvent, organic binder, and glass frit. The size of the Cu powder particles was 3 μm or below. The viscosity of the Cu paste was 6.3 Pa s. The Seebeck coefficient of the $CoSb_3$ film annealed at 500°C was -49 μV/K at 500 K operational temperature. This value is lower than the reported value using bulk $CoSb_3$,[12] as our process conditions for $CoSb_3$ are not fully optimized. The resistivity of the $CoSb_3$ film annealed at 500°C was 4.75×10^{-3} Ω cm. This value is similar to the case of bulk $CoSb_3$ (6×10^{-3}–4×10^{-2} Ω cm). We are currently working on $CoSb_3$ film to improve the thermoelectric properties.

Figure 5 shows the process flow of the thermoelectric module obtained using screen-printing technology. An illustration of the process sequence and pictures of a fabricated thermoelectric module are also presented in this figure. Patterned Cu pad metals were first formed on both the top and bottom of an alumina substrate by screen-printing and annealing. No photolithography process is involved here. ZnSb and $CoSb_3$ were then formed as *p*-type and *n*-type thermoelectric legs, respectively, on the Cu metal pads on the top and bottom substrates, respectively. Finally, the top and bottom substrates were bonded by Cu paste. A photograph of the fabricated thermoelectric module is presented in Fig. 5d. Further optimization of all device parameters such as thermoelectric material thickness, size, and packing density of films should be carried out in future work. In our device, the film thickness can be controlled by adjusting the paste viscosity, the distance between the squeegee and the mask, the mesh size of the screen mask, and the squeegee speed during the screen-printing process. The pattern size can be easily controlled by the use of various screen masks.

Figure 6 shows the output voltage and power of the thermoelectric module fabricated with the proposed screen-printing technique. The fabricated thermoelectric module has legs of two couples. The size of the leg is 5 mm × 5 mm × 50 μm, and the distance between the thermoelectric legs is 5 mm, which can be further optimized. Output voltage and output power per unit area at a temperature difference of 50 K were 27 mV and 0.1 mW/cm^2, respectively. These values are lower than anticipated from the output characteristics of the ZnSb

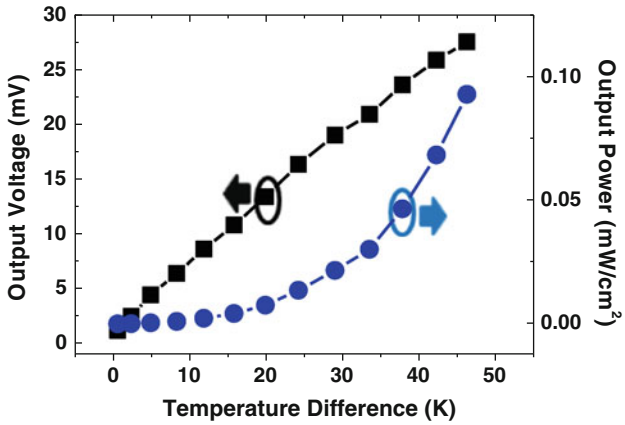

Fig. 6. Output voltage and power of the thermoelectric module fabricated by the proposed screen-printing technique.

film shown in Fig. 4. This is attributed to the structure not having been optimized and to the high contact resistance caused by the nonoptimized bonding process.

CONCLUSIONS

A screen-printing technique was successfully used to fabricate a thermoelectric module with low cost per watt. A thermoelectric module using ZnSb and $CoSb_3$ as *p*-type and *n*-type thermoelectric legs, respectively, was fabricated. The screen-printing process is a simple and low-cost process and is suitable for mass production, and the materials employed here are abundant, inexpensive, and nontoxic. The approach presented in this paper shows good feasibility for producing low-cost thermoelectric modules, which are attractive for renewable, green energy applications.

ACKNOWLEDGEMENTS

This work was supported by the Ministry of Knowledge Economy (MKE), Korea, under the ITRC program supervised by the National IT Industry Promotion Agency (NIPA) [NIPA-2009-(C1090-0904-0007)], and the Fusion Research Program for Green Technologies through the National Research Foundation of Korea (NRF) funded by the Ministry of Education, Science, and Technology (2010-0019085).

REFERENCES

1. G. Jeffrey Snyder and E.S. Toberer, *Nat. Mater.* 7, 105 (2008).
2. A.L. Vayner, *Mosc.* (1983), p. 30.
3. D. Astrain, J.G. Vián, and M. Domínguez, *Appl. Therm. Eng.* 23, 2183 (2003).
4. R. Venkatasubramanian, E. Siivola, T. Colpitts, and B. O'Quinn, *Nature* 413, 597 (2001).
5. B.J. Huang, C.J. Chin, and C.L. Duang, *Int. J. Refrig.* 23, 208 (2000).
6. M. Yamanashi, *J. Appl. Phys.* 80, 5494 (1996).
7. S. Goktun, *Energ. Source* 18, 531 (1996).
8. F.D. Rosi, *Solid State Electron* 11, 833 (1968).
9. G. Min and D.M. Rowe, *J. Power Sources* 38, 253 (1992).
10. D.M. Rowe and G. Min, *J. Power Sources* 73, 193 (1998).
11. B.I. Ismail and W.H. Ahmed, *Recent Pat. Electr. Eng.* 2, 27 (2009).
12. Y. Kawaharada, K. Kurosaki, M. Uno, and S. Yamanaka, *J. Alloys Compd.* 315, 193 (2001).